REPORT DOCUMENTATION PAGE

Form Approved
OMB NO. 0704-0188

1. AGENCY USE ONLY (Leave Blank)	2. REPORT DATE 3/22/2004	3. REPORT TYPE AND DATES COVERED final progress report, 6/12/2000-12/31/2003

4. TITLE AND SUBTITLE
Optical processes in high-Q semiconductor microcavities

5. FUNDING NUMBERS
DAAD19-00-01-0393

6. AUTHOR(S)
Hailin Wang

7. PERFORMING ORGANIZATION NAME(S) AND ADDRESS(ES)
University of Oregon
Department of Physics
Eugene, OR 97403-1274

8. PERFORMING ORGANIZATION REPORT NUMBER

9. SPONSORING / MONITORING AGENCY NAME(S) AND ADDRESS(ES)
U. S. Army Research Office
P.O. Box 12211
Research Triangle Park, NC 27709-2211

10. SPONSORING / MONITORING AGENCY REPORT NUMBER
40671-PH-QC

11. SUPPLEMENTARY NOTES
The views, opinions and/or findings contained in this report are those of the author(s) and should not be construed as an official Department of the Army position, policy or decision, unless so designated by other documentation.

12 a. DISTRIBUTION / AVAILABILITY STATEMENT
Approved for public release; distribution unlimited.

12 b. DISTRIBUTION CODE

13. ABSTRACT (Maximum 200 words)

This final progress report summarizes research efforts in two areas: cavity QED of quantum dots and electromagnetically induced transparency (EIT) in GaAs quantum wells. Cavity QED studies are based on the development of a composite nanocrystal-microsphere system, in which CdSe/ZnS core/shell nanocrystals couple to whispering gallery modes (WGMs) in a fused silica microsphere. The composite microcavity system can feature a Q-factor as high as 10^8 and a nanocrystal decoherence rate as small as 3 μeV (0.75 GHz), indicating that the composite system can in principle reach the strong coupling regime of cavity QED. EIT studies have exploited the use of Coulomb interactions between excitons to induce and manipulate exciton spin coherence and biexciton coherence. These studies have led to the first experimental demonstration of EIT in inter-band optical transitions in semiconductors in Λ-type, cascaded, and V-type three-level systems.

14. SUBJECT TERMS
Cavity QED, nanocrystals, whispering gallery modes, spin coherence, biexciton coherence, electromagnetically induced transparency (EIT)

15. NUMBER OF PAGES
14

16. PRICE CODE

17. SECURITY CLASSIFICATION OR REPORT	18. SECURITY CLASSIFICATION ON THIS PAGE	19. SECURITY CLASSIFICATION OF ABSTRACT	20. LIMITATION OF ABSTRACT
UNCLASSIFIED	UNCLASSIFIED	UNCLASSIFIED	UL

Final Progress Report

Optical processes in high-Q semiconductor microcavities

June 12, 2000 to Dec. 31, 2003

Principal Investigator:	Hailin Wang Associate Professor Department of Physics University of Oregon Eugene, OR 97403 Voice 541-346-4758 Fax 541-346-4315 hailin@oregon.uoregon.edu
Institution:	University of Oregon Research Service and Administration Eugene, OR 97403-5215

Grant Number:	DAAD19-00-01-0393
ARO Proposal Number:	P-40671-PH-QC

TABLE OF CONTENTS

1. Statement of problems studied

a) Composite nanocrystal-microsphere system

We have proposed a composite nanocrystal-microsphere system to implement scalable cavity-QED based quantum logic gates [1]. In this scheme, an array of semiconductor nanocrystals is deposited on the equator of a high-Q fused silica microsphere. A two-level system consisting of the ground state and a metastable excited state of a nanocrystal serves as a qubit. Coherent interactions between two qubits are mediated by a photon in a high-Q whispering gallery mode (WGM). For the quantum logic operation, the composite system needs to reach the strong-coupling regime, in which the dipole-coupling rate between a nanocrystal and a single photon in the cavity mode exceeds both the cavity decay rate and the nanocrystal decoherence rate. Our research efforts have focused on the fabrication and characterization of the composite nanocrystal-microsphere system and on the measurement and understanding of intrinsic decoherence processes in semiconductor nanocrystals.

We fabricated the composite nanocrystal-microsphere system by depositing CdSe/ZnS core/shell nanocrystals on the surface of a fused silica microsphere. The composite system can feature a Q-factor near 10^8, which is a few orders of magnitude greater than that of other semiconductor microcavity systems [2, 3]. Using techniques based on high-resolution spectral hole burning, we obtained intrinsic decoherence rates as small as 0.75 GHz (3 μeV) in CdSe/ZnS core/shell nanocrystals, more than one order of magnitude smaller than previously reported [4, 5]. The small decay rates for both the cavity mode and the quantum coherence in nanocrystals have in principle put the composite nanocrystal-microsphere system in the strong-coupling regime. Nevertheless, rapid fluctuations in the nanocrystal transition frequency have prevented us from directly demonstrating the effects of strong coupling. The difficulties we encounter illustrate the daunting challenges in engineering a well-isolated solid-state system for quantum information processing. In our case, the movement of a single electron on the nanocrystal surface can kick the nanocrystal out of resonance with the cavity mode.

b) Electromagnetically induced transparency in semiconductors

We have initiated an experimental program to realize electromagnetically induced transparency (EIT) in semiconductors. EIT is a phenomenon that exploits destructive interference induced by a nonradiative quantum coherence to render an opaque medium transparent [6]. EIT studies in atomic systems have led to the demonstration and discovery of a number of remarkable phenomena, including slow light, stored light (storing quantum information of light as stationary spin coherence), and entangled light (entangled photon pairs with a well-defined delay) [7]. These phenomena have important applications in both classical (e.g., optical buffers) and quantum information processing (e.g., quantum memory of photons and entangled photon pairs for quantum communication) [8].

To realize EIT in semiconductors, we have developed novel schemes based on the use of exciton spin coherence and biexciton coherence in GaAs quantum wells [9-11]. Exciton spin

coherence is a coherent superposition of the exciton spin states and is induced in our experimental study via exciton-exciton scattering in a two-exciton continuum, which is quite unusual since such scattering processes were believed to destroy instead of inducing quantum coherences. Biexciton coherence is a coherent superposition between the crystal ground state and a bound state of two excitons. Both of these coherences arise from Coulomb interactions between excitons and have no counterparts in independent atomic systems. The use of these quantum coherences has led to the first demonstration of EIT in interband optical transitions in semiconductors. It should be noted that a central issue in manipulating quantum coherences in semiconductors is that manybody Coulomb interactions between optical excitations such as excitons can fundamentally alter the behaviors of these coherences. Our EIT studies illustrate that in a counter-intuitive way, an effective approach to manipulate and use quantum coherences in semiconductors is to harness instead of avoiding manybody Coulomb interactions.

2. Summary of the most important results

a) Composite nanocrystal-microsphere system

We have developed a quantum-dot microcavity system that couples semiconductor nanocrystals to a fused silica microsphere [2, 3]. The new microcavity system takes advantage of the high Q-factor and the small mode volume of WGMs in the fused silica microsphere and also allows separate engineering of electronic and photonic components of a cavity-QED system. Fused silica microspheres were fabricated by fusing the tip of a tapered optical fiber with a focused CO_2 laser beam. The size of the sphere can range from 5 μm to a few hundred μm. Figure 1a shows the image of a fused silica microsphere with CdSe/ZnS core/shell nanocrystals deposited on the sphere surface through solution deposition. The bright red photoluminescence from nanocrystals on the sphere surface can be seen clearly.

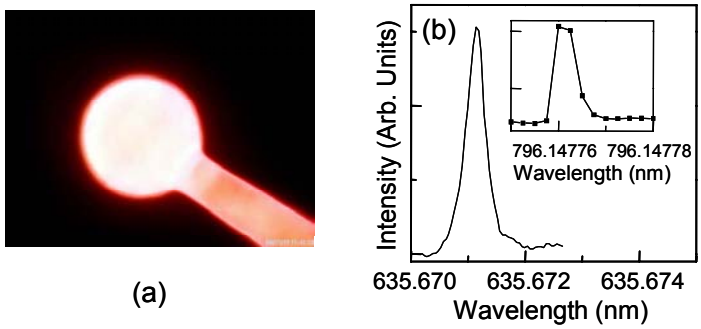

Fig. 1 a) A fused silica microsphere with CdSe nanocrystals deposited on the surface. b) WGM resonance near and far below (the inset) the exciton absorption line center. The result in the inset is limited by the scanning step size of the laser. The diameter of the sphere is near 100 μm.

We characterized the composite nanocrystal-microsphere system by using a resonant light scattering technique, in which WGMs were directly excited via frustrated internal reflection in a high index optical prism. Figure 1b shows the resonant scattering spectra obtained near the absorption line center of the nanocrystals and also far below the band gap (see the inset). Near the absorption line center, the spectral linewidth of the WGM is 4×10^{-4} nm, corresponding to a

Q-factor of 1.6×10^6. Far below the band gap, the linewidth decreases to 5×10^{-6} nm (~ 2 MHz), corresponding to a Q-factor of 1.6×10^8 and a cavity finesse of 1.4×10^5. This difference in the Q-factors is due to absorption of nanocrystals coupling to the relevant WGMs. Separate time-domain ring-down spectroscopy has further shown that the intrinsic Q-factor of the composite nanocrystal-microsphere system is limited to a few times of 10^8 by surface adsorption of chloroform solution used in the nanocrystal deposition process.

We investigated intrinsic decoherence rates in CdSe/ZnS core/shell nanocrystals using the technique of high-resolution spectral hole burning (SHB) [4, 5]. SHB responses from CdSe/ZnS core/shell nanocrystals obtained at 10 K (see Fig. 2) feature a sharp resonance at zero pump-probe detuning as well as additional sidebands arising from optical transitions assisted by absorption or emission of confined acoustic phonons. The energy positions of the phonon sidebands are in general agreement with the theoretically calculated confined phonon energy (see the inset in Fig, 2). The quantization of acoustic phonon modes in a nanocrystal eliminates pure dephasing induced by coupling of excitons to a continuum of acoustic phonon modes.

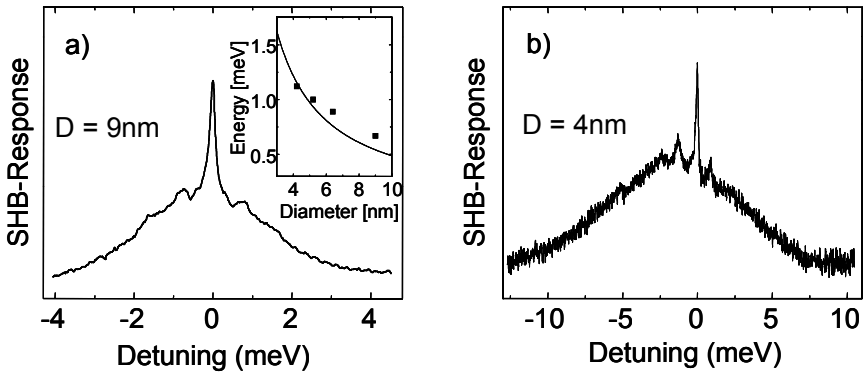

Fig. 2 SHB response obtained at T=10K and a modulation frequency of 20 kHz. (a) D=9 nm. (b) D=4 nm. The inset shows the size dependence of the energy separation between the SHB resonance and the first sideband. The solid line is the calculated energy for confined acoustic phonons with l=2 and n=1 [5].

A major difficulty in determining the intrinsic decoherence rate of semiconductor nanocrystals is spectral diffusion: random spectral shifts in the optical transition frequency due to fluctuating microscopic local environment. In the limit that the measurement timescale is slow or comparable to the timescale of spectral diffusion, spectral diffusion processes can significantly broaden the nanocrystal absorption resonance. As a result, the SHB linewidth becomes dependent on the measurement timescale. For the SHB study, the timescale of the measurement is set by the modulation period used in the lock-in detection. Figure 3a shows that at relatively low modulation frequencies, the SHB linewidth decreases drastically with increasing modulation frequency, revealing a dominant contribution to the SHB linewidth from spectral diffusion. The SHB linewidth obtained at modulation frequencies of a few MHz approaches an asymptotic value. Figure 3b is an example of an expanded scan of the SHB resonance obtained at a modulation frequency of Ω=1 MHz. By eliminating effects of spectral diffusion with high modulation frequency, we are able to obtain intrinsic decoherence rates as small as 3 μeV (0.75 GHz) in CdSe/ZnS core/shell nanocrystals, more than one order of magnitude smaller than

previously reported. Note that in the absence of spectral diffusion, the linewidth of the SHB resonance is four times the intrinsic decoherence rate.

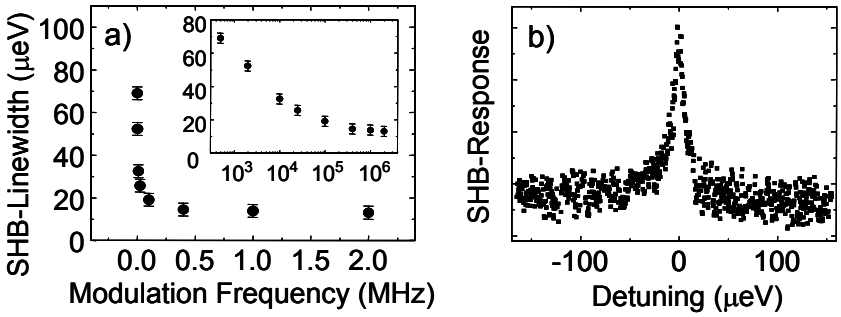

Fig. 3 (a) Modulation frequency dependence of the SHB linewidth with $I_{pump}=I_{probe}=0.5W/cm^2$. The inset shows the same data in logarithmic scale. (b) An expanded scan of a SHB resonance obtained at Ω =1 MHz. All data were obtained at T=2 K and for nanocrystals with *D*=9 nm.

The decay rates for both the cavity mode and the quantum coherence in nanocrystals are small compared with the theoretically estimated dipole-coupling rate, indicating that the composite nanocrystal-microsphere system can in principle reach the strong-coupling regime. Nevertheless, rapid spectral diffusion in the nanocrystal transition frequency as revealed in Fig. 3a has prevented us from demonstrating the effects of strong coupling. A major challenge is to further improve the surface properties of the nanocrystal to eliminate or suppress local environmental fluctuations.

b) Electromagnetically induced transparency in semiconductors

We have developed a number of novel schemes that exploit the use of strong Coulomb interactions between excitons to induce and manipulate nonradiative quantum coherences. We have successfully demonstrated EIT using exciton spin coherence, biexciton coherence, and intervalence band coherence in GaAs quantum wells (QWs). Using EIT from a biexciton coherence, we have achieved a 20-fold reduction in the absorption of an exciton resonance in GaAs QWs. These studies demonstrate, for the first time, EIT of interband optical transitions in semiconductors and open the door to further exploration of EIT in a wide variety of applications including coherent spin manipulation, quantum information processing, and photonics and nonlinear optics.

EIT is typically realized in a 3-level system (see Fig. 4) where a control beam drives the |2> to |3> transition and sets up a destructive quantum interference for a weak probe or signal beam coupling to the |1> to |2> transition. Experimentally, the induced transparency becomes observable when Ω_c exceeds both γ_{13} and $\sqrt{\gamma_{13}\gamma}$, where Ω_c is the Rabi frequency of the control beam and γ and γ_{13} are decay rates of the relevant dipole coherence and the nonradiative coherence between states |1> and |3>, respectively. The induced transparency is also accompanied by a steep dispersion in the refractive index, leading to large reductions in the group velocity of light (slow light).

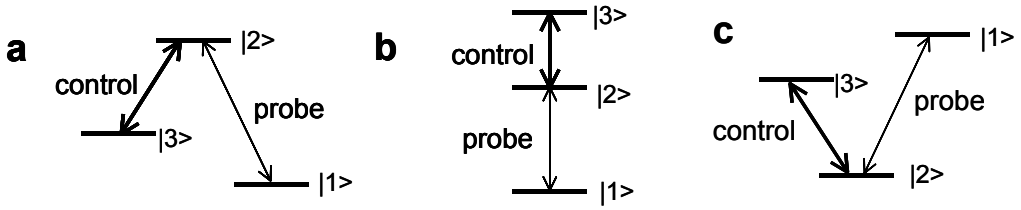

Fig. 4. EIT schemes in Λ-type, cascaded-type, and V-type 3-level systems, respectively.

We have successfully demonstrated EIT in semiconductors with all three types of three-level systems shown in Fig. 4, specifically, EIT from exciton spin coherence (Λ-type) [9, 11], biexciton coherence (cascaded-type) [10], and intervalence coherence (V-type) [12]. Experimental studies were all carried out at 10 K.

i) EIT from exciton spin coherence

The lowest energy inter-band optical transition in III-V semiconductors such as a GaAs QW is between the doubly degenerate conduction bands with spin s=±1/2 and the doubly degenerate heavy-hole (hh) valence bands with total angular momentum components m_j=±3/2 (Fig. 5a). Using circularly polarized light, we can excite spin-up (via σ + transition) and spin-down (via σ – transition) excitons. While these two transitions share no common states, correlations caused by the Coulomb interaction between excitons with opposite spins can lead to the formation of bound two-exciton (exciton molecule or biexciton) states as well as unbound two-exciton continuum states (Fig. 5b). We have exploited the use of these two-exciton states to induce nonradiative quantum coherences, including exciton spin coherence (a coherent superposition of spin-up and spin-down exciton states) and biexciton coherence (a coherent superposition of the ground and the biexciton states), and have used these nonradiative coherences to successfully realize EIT in semiconductors.

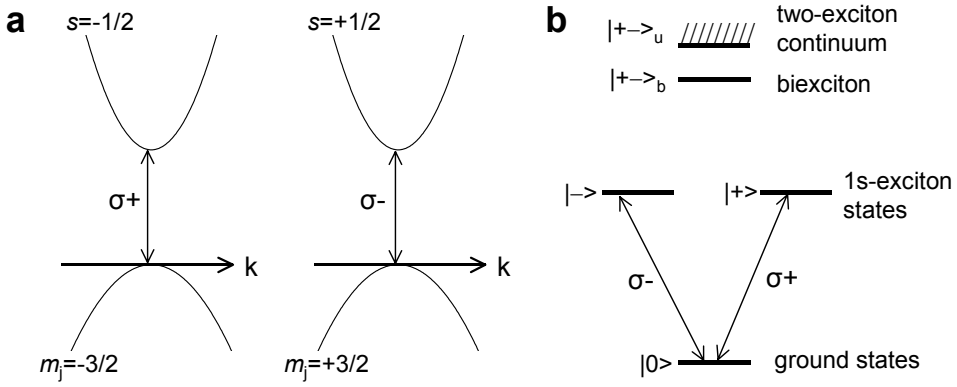

Fig. 5 (a) The degenerate conduction bands and hh valence bands a GaAs QW along with the selections rules. (b) Schematic of energy eigenstates for the ground, one exciton, and two-exciton states where |+>, |–>, $|+->_b$, $|+->_u$ represent the spin-up and spin-down one-exciton states, and the bound and unbound two-exciton states, respectively.

As shown in Fig. 6, |+>, |–> and $|+->_b$ realizes a Λ-type three-level system. We prepared the system and populated the |+> state by using a σ+ polarized prepulse that is resonant with the

excitonic transition. For the EIT experiment (see Fig. 6), a strong control pulse (6 ps in duration) coupling to the |–> to $|+-\rangle_b$ transition along with a weak probe pulse (150 fs in duration) coupling to the |+> to $|+-\rangle_b$ transition set up an exciton spin coherence. Absorption spectra and the EIT in the |+> to $|+-\rangle_b$ transition were measured by spectrally resolving the probe pulse after its transmission through the sample. The energy flux of the probe pulse was kept at 1/100 that of the control pulse.

Figure 6 shows the experimental results obtained in a GaAs/AlGaAs QW with 10 periods of 10 nm GaAs wells. The dotted curve in Fig. 6a shows the biexciton resonance, corresponding to the |+> to $|+-\rangle_b$ transition, obtained in the absence of the control pulse. This resonance is induced by the incoherent pumping from the prepulse and vanishes without the prepulse. A pronounced absorption dip occurs in the biexcitonic resonance when the control pulse and the probe pulse have the opposite circular polarization, as shown in the solid curve in Fig. 6a. The dip in Fig. 6a vanishes when the probe pulse arrives a few ps after the control pulse while the biexcitonic resonance still persists, as shown in Fig. 6b. This absorption dip arises from destructive interference associated with the spin coherence, thus demonstrating EIT from the exciton spin coherence. The degree of transparency is limited by the rapid decay of the exciton spin coherence.

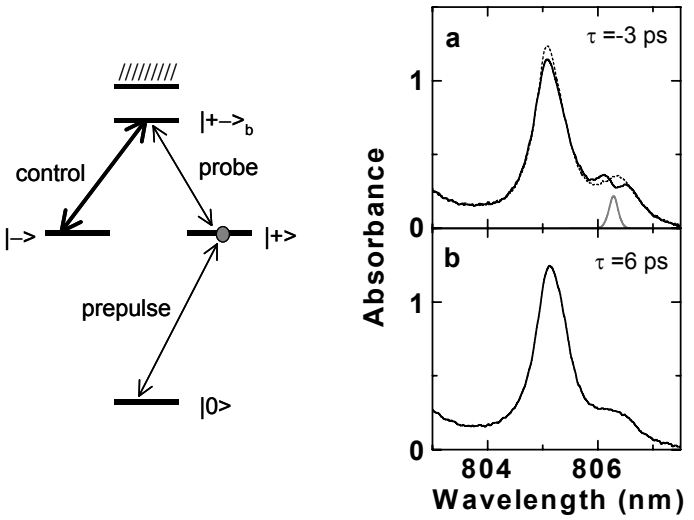

Fig. 6 Absorption spectra measured by the probe pulse in the absence (dotted lines) and presence (solid lines) of the control pulse at 10 K. The spectrum of the control pulse is shown in the bottom of Fig. 6a. Negative delay means that the probe pulse arrives before the peak of the control pulse. The control pulse energy flux is 800 nJ/cm^2.

The exciton spin coherence can be induced not only via the bound two-exciton state but also via the two-exciton continuum states. Figure 7 shows the experimental results where the control pulse excited a polarization of spin-up excitons and also coupled to the |–> to $|+-\rangle_u$ transition. In this case, the coupling of the control to the |–> to $|+-\rangle_u$ transition, along with the coupling of the probe to the |+> to $|+-\rangle_u$ transition, excited an exciton spin coherence via the two-exciton continuum states. The resulting EIT occurs at the exciton energy and satisfies the two-photon resonance condition of the spin coherence, as shown by the spectral position of the absorption dip in Fig. 7. The dip vanished when the probe was delayed a few ps after the control and was the most pronounced when the probe slightly preceded the control, which is

characteristic of this type of coherent transient optical processes and rules out spectral hole burning as a possible mechanism. The success of realizing EIT via exciton spin coherence has also paved the way for our current effort of realizing EIT by using the more robust electron spin coherence [13, 14].

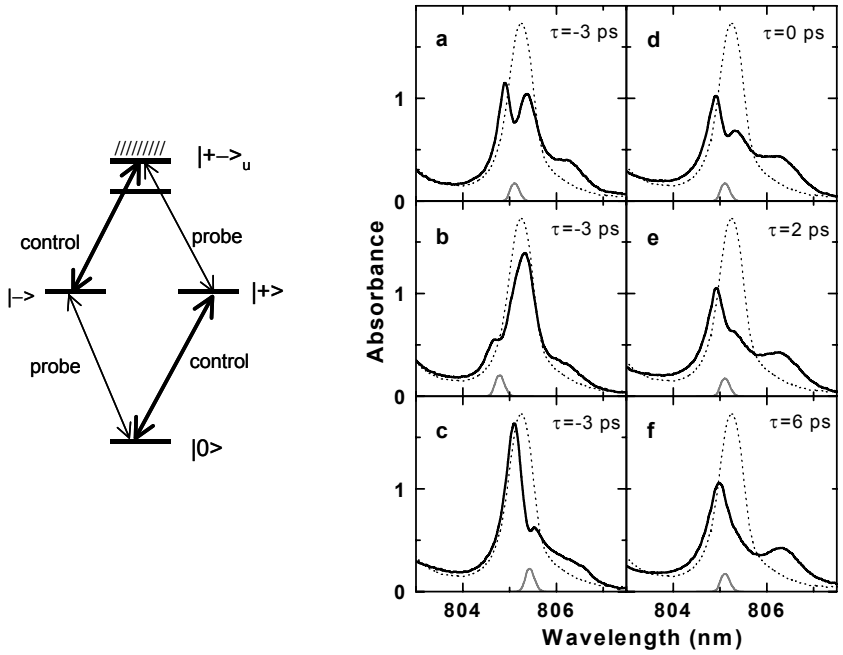

Fig. 7 Absorption spectra measured by the probe pulse in the absence (dotted lines) and presence (solid lines) of the control pulse. The spectrum of the pump is shown in the bottom of each figure. The control pulse energy flux is 400 nJ/cm^2.

ii) EIT from biexciton coherence

As shown in Fig. 8, |0>, |–> and $|+->_b$ realizes a cascaded three-level system. In this case, the destructive quantum interference can be set up by a control pulse that couples to the exciton-to-biexciton transition. Figures 8a and 8b show the absorption spectra measured by the probe with the control pulse at two different spectral positions in a GaAs/AlGaAs QW with 15 periods of 17.5 nm GaAs wells. The largest reduction in the exciton absorption was obtained when the control pulse was between the exciton and biexciton resonances. In this case, the EIT dip occurred at the energy of the hh exciton resonance and the absorption at the EIT dip was reduced by more than 20-fold [the reduction in αL is 3.1, corresponding to a decrease in absorption of exp(3.1) = 22]. In comparison, when the control pulse was at the biexciton resonance, only a modest reduction in the absorption of the exciton resonance was observed and the EIT dip occurred at an energy slightly higher than the hh exciton resonance. Figure 8c also shows the absorption spectrum obtained with the probe arriving 10 ps after the control. The spectrum is nearly identical to the linear absorption spectrum obtained in the absence of the control pulse, indicating minimal real absorption of the control pulse. This nearly complete recovery of the absorption spectrum further confirms that the reduction in the absorption of the exciton resonance is EIT in origin with minimal contributions from incoherent bleaching.

For the above experiments, the EIT dip shifted to lower energy when the control pulse was tuned to higher energy, consistent with the two-photon resonance condition expected for the EIT

process. The spectral positions of the EIT dips, however, do not exactly correspond to those expected for an atomic-like system. This unusual behaviour arises from a shift in the spectral position of the biexciton resonance due to interactions between excitons and biexcitons. To realize strong EIT processes, it is crucial that the effects of the exciton-biexciton interactions be pre-compensated by adjusting the spectral position of the control pulse, as shown in Fig. 8a. The above experimental results can be described quantitatively by a microscopic theory developed by the Binder group at the University of Arizona. The theory is based on the dynamics controlled truncation formalism extended beyond the $\chi^{(3)}$ limit.

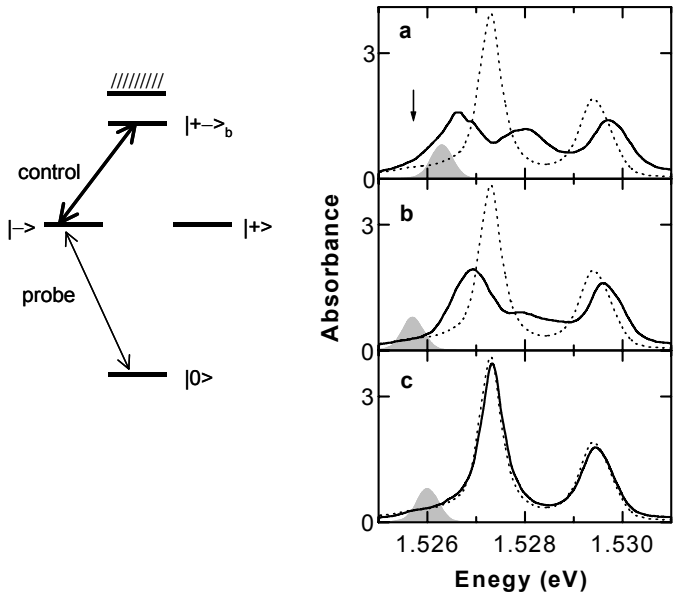

Fig. 8 Absorption spectra measured by the probe pulse in the absence (dotted lines) and presence (solid lines) of the control pulse at 10 K. Shaded areas show spectra of the control pulse. The arrow indicates the position of the biexciton resonance. The probe pulse arrives 1 ps before the peak of the control pulse for (a) and (b) and 10 ps after the peak of the control pulse for (c). The control pulse energy flux is 400 nJ/cm^2.

iii) EIT from intervalence band coherence

EIT can also be induced via a coherence between two valence bands. For III-V semiconductors such as a GaAs QW, the valence bands are characterized by the two hh bands with m_j=±3/2 and also the two light hole (lh) bands with m_j=±1/2. As shown schematically in Fig. 9a, the hh excitonic transition with σ+ circular polarization and the lh excitonic transition with σ– circular polarization share a common conduction band state. A nonradiative coherence between the two valence bands can be induced via these two transitions. Note that the hh and lh excitonic transitions do not form a Λ-type 3-level system since both valence bands are initially occupied. These transitions should be viewed as a V-type three-level system, as shown schematically by the exciton energy diagram in Fig. 9b. Destructive interference associated with the intervalence band coherence can lead to EIT in the V-type three-level system.

To induce the coherence between the hh and lh valence bands, we applied a control pulse with σ+ polarization and with an energy flux per pulse of 160 nJ/cm^2 to the hh excitonic transition. Figure 9c shows absorption spectra measured by a probe pulse in the presence of the control with the same (dashed line) and the opposite (solid line) circular polarization in a GaAs/AlGaAs QW with 8 periods of 13 nm GaAs wells. When the control and probe had the

same circular polarization, Rabi splitting of the hh exciton transition was observed. When the pump and probe had the opposite circular polarization, an absorption dip (marked by the arrow in the figure) in the lh exciton resonance was observed. The dip satisfies the two-photon resonance condition for the intervalence band coherence. Note that a more pronounced absorption dip also appeared in the hh exciton resonance. The dips in both the hh and lh resonances vanished when the probe pulse was delayed more than a few ps with respect to the control pulse, ruling out spectral hole burning as a possible mechanism. The dip in the lh resonance is due to EIT induced by the intervalence band coherence while the dip in the hh resonance is due to EIT arising from the exciton spin coherence discussed earlier. The EIT dip in the lh exciton resonance is also in good agreement with a numerical calculation based on the V-type three-level system. The degree of transparency, however, is limited by the rapid decay of the intervalence band coherence.

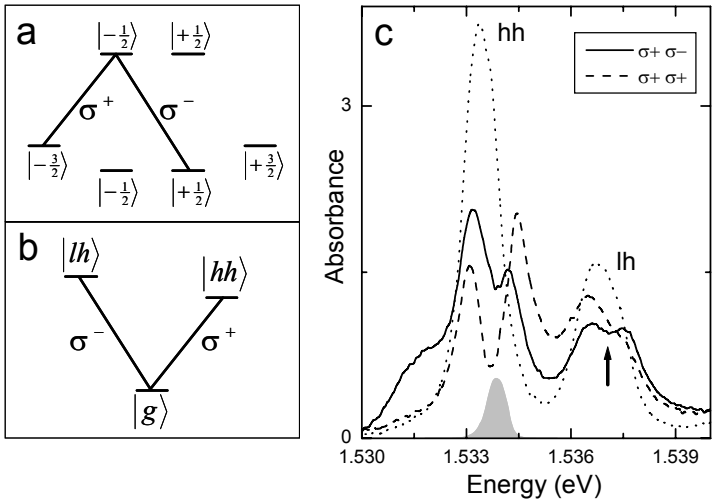

Fig. 9 (a) Intervalence band coupling. (b) V-type three-level system where |hh> and |lh> are the heavy-hole and light-hole exciton states, respectively. (c) Absorption spectra of a σ− probe in the absence (dotted) and in the presence of a control pulse resonant with the hh exciton and with σ+ (solid) and σ− (dashed) polarization. The arrow indicates the EIT dip in the lh exciton resonance.

3. Publication

JOURNAL ARTICLES:

Phedon Palinginis and Hailin Wang, "*High-resolution spectral hole burning in CdSe/ZnS core/shell nanocrystals*," Appl. Phys. Lett. **78**, 1541 (2001).

Mark Phillips and Hailin Wang, "*Spin coherence and electromagnetically induced transparency via exciton correlations*," Phys. Rev. Lett. **89**, 186401 (2002).

Phedon Palinginis, Sahsa Tavenner, Mark Lonergan, and Hailin Wang, "*Spectral hole burning and zero-phonon linewidth in semiconductor nanocrystals,"* Phys. Rev. B**67** Rapid Comm., 201307 (2003).

Mark Phillips and Hailin Wang, "*Electromagnetically induced transparency due to intervalence band coherence in semiconductors,"* Optics Lett. **28**, 831 (2003).

Mark Phillips, Hailin Wang, I. Rumyantsev, N.H. Kwong, R. Takayama, and R. Binder, "*Electromagnetically induced transparency in semiconductors via biexciton coherence,"* Phys. Rev. Lett. **91**, 183602 (2003).

Tao Li, Hailin Wang, N.H. Kwong, and R. Binder, "*Electromagnetically induced transparency from electron spin coherence in a quantum well waveguide,"* Opt. Express **11**, 3298 (2003).

Phedon Palinginis and Hailin Wang, "*Vanishing and emerging of absorption quantum beats from electron spin coherence in GaAs quantum wells,"* Phys. Rev. Lett. **92**, 037402 (2004).

Mark Phillips and Hailin Wang, "*Exciton spin coherence and electromagnetically induced transparency in the transient optical response of GaAs quantum wells*," Phys. Rev. B (in press).

BOOK CHAPTER:

Hailin Wang, "*Cavity QED of quantum dots with dielectric microsphere*," in Coherence, Correlations, and Decoherence in Semiconductor Nanostructures, edited by T. Takagahara (Academic Press, 2003).

INVITED PRESENTATIONS AT INTERNATIONAL CONFERENCES AND WORKSHOPS:

Controlling optical interactions in semiconductor microcavities using whispering gallery optical cavities, American Physical Society March Meeting, Seattle (March 2001).

Cavity QED of quantum dots with dielectric microspheres, Fundamental Optical Processes in Semiconductors, Girdwood, Alaska (August 2001).

Spin coherence via exciton correlations, The fourth annual meeting of the Southwest Quantum Information and Technology Network (March 2002).

Dephasing and cavity QED of semiconductor nanocrystals, Second International Conference on Quantum Dots, Tokyo, Japan, (Sept. 2002).

C*avity QED of semiconductor nanocrystals*, International Symposium on Nanotechnology for Photonics and Optoelectronics, Tokyo, Japan (March, 2003).

Dipole and spin coherence in semiconductor nanostructures, Joint US-Australia Workshop on Solid State and Optical Approaches to Quantum Information Science, Sidney (Jan. 2003).

Cavity QED of semiconductor nanocrystals, Miami University Nanotechnology Center Inaugural Symposium (Nov. 2003).

Electromagnetically induced transparency from spin coherences in semiconductors, DARPA Slow Light Workshop, Orlando (Dec. 2003).

Electromagnetically induced transparency via exciton correlations, Photonics West, San Jose (Jan. 2004)

Electromagnetically induced transparency from spin coherences in semiconductors, Plenary talk, Physics of Quantum Electronics, Snowbird Utah (Jan. 2004).

Electromagnetically induced transparency from spin coherences in semiconductors, International Quantum Electronics Conference, San Francisco (May 2004).

EXTENDED CONFERENCE SUMMARIES (REFEREED):

Phedon Palingnis, Sasha Tevenner, Hailin Wang, and Mark Lonergan, "*Homogeneous linewidth in CdSe/ZnS core/shell nanocrystals*," Quantum Electronics and Laser Sciences Conference, QELS'01, Baltimore, MD (June 2001).

Phedon Palinginis and Hailin Wang, "*Dephasing and light-induced spectral diffusion in CdSe/ZnS core/shell nanocrystals*," Quantum Electronics and Laser Sciences Conference, QELS'02, Long Beach, CA (May, 2002).

Mark Phillips and Hailin Wang, "*Exciton Rabi splitting in semiconductor quantum wells*," Quantum Electronics and Laser Sciences Conference, QELS'02, Long Beach, CA (May, 2002).

Hailin Wang and Mark Phillips and, "*Exciton spin coherence via Coulomb correlations*," Quantum Electronics and Laser Sciences Conference, QELS'03, Baltimore (June, 2003).

Mark Phillips, Hailin Wang, I. Rumyantsev, N.H. Kwong, R. Takayama, and R. Binder, "*Electromagnetically induced transparency via biexciton coherence,"* Quantum Electronics and Laser Sciences Conference, QELS'03, Baltimore (June, 2003).

Phedon Palinginis, Hailin Wang, and Jacek Furdyna "*Dephasing and spectral hole burning in self-assembled CdSe quantum dots*," Quantum Electronics and Laser Sciences Conference, QELS'03, Baltimore (June, 2003).

Phedon Palinginis and Hailin Wang, "*Coherent Raman resonance from electron spin coherence in GaAs quantum wells"*, International Conference of Magnetism, Rome (Aug. 2003).

4. Scientific Personnel

Mark Phillips (graduate student)
Phedon Palinginis (graduate student)
Sasha Tevenner (graduate student)
Susanta Sarkar (graduate student)
Yumin Shen (graduate student)
Yao Li (graduate student)
Hailin Wang (PI)

Mark Phillips successfully defended his PhD thesis entitled "Electromagnetically induced transparency in semiconductor" in 2002 and is now a postdoctoral staff scientist at Sandia National Laboratories.

Phedon Palinginis is scheduled to defend his PhD thesis in April 2004.

5. Report of inventions

No patents were filed.

6. Bibliography

1) T. A. Brun and Hailin Wang, Phys. Rev. A**61**, 323071 (2000).

2) Xudong Fan, Scott Lacey, Phedon Palinginis, Hailin Wang, and Mark Lonergan, Opt. Lett. **25**, 1600 (2000).

3) Hailin Wang, "*Cavity QED of quantum dots with dielectric microsphere*," in Coherence, Correlations, and Decoherence in Semiconductor Nanostructures, edited by T. Takagahara (Academic Press, 2003).

4) Phedon Palinginis and Hailin Wang, Appl. Phys. Lett. **78**, 1541 (2001).

5) Phedon Palinginis, Sasha Tavenner, Mark Lonergan, and Hailin Wang, Phys. Rev. B**67** Rapid Comm., 201307 (2003).

6) S.E. Harris, Phys. Today **50(7)**, 36-42 (1997); M.O. Scully, and M.S. Zubairy, *Quantum Optics* (Cambridge Univ. Press, Cambridge, 1997); E. Arimondo, in *Progress in Optics* (ed. Wolf, E.) **35**, 259-354 (North-Holland, Amsterdam, 1996).

7) For a recent review, see for example, M. Lukin, Rev. Mod. Phys. **75**, 457 (2003).

8) See for example, L. M. Duan, M.D. Lukin, J.I. Cirac, P. Zoller, Nature **414**, 413 (2001).

9) Mark Phillips and Hailin Wang, Phys. Rev. Lett. **89**, 186401 (2002).

10) Mark Phillips, Hailin Wang, I. Rumyantsev, N.H. Kwong, R. Takayama, and R. Binder, Phys. Rev. Lett. **91**, 183602 (2003).

11) Mark Phillips and Hailin Wang, Phys. Rev. B, accepted for publication.

12) Mark Phillips and Hailin Wang, Optics Lett. **28**, 831 (2003).

13) Tao Li, Hailin Wang, N.H. Kwong, and R. Binder, Opt. Express **11**, 3298 (2003).

14) Phedon Palinginis and Hailin Wang, Phys. Rev. Lett. **92**, 037402 (2004).